M. D. Wuestling

S. A. Klein

J. A. Duffie

Solar Energy Laboratory,
University of Wisconsin-Madison,
1500 Johnson Drive,
Madison, Wisc. 53706

Promising Control Alternatives for Solar Water Heating Systems

Although the performance of solar domestic hot water (SDHW) systems has been well studied, there are several promising control alternatives that have not been thoroughly investigated. Reduced constant collector fluid flow rates, variable collector flow rates, and variable volume storage are several alternative strategies. This paper presents the results of an analytical study using the TRNSYS simulation program in which the thermal performance of SDHW systems utilizing alternative control strategies are compared while operating under realistic conditions in several different climates of the United States. The effects on system performance of time of year, collector area and quality, preheat storage tank volume and energy losses, occurrence of mixing the preheat storage tank, controller temperature deadbands, auxiliary set temperature, total daily usage, and load distribution are investigated.

1 Introduction

Conventional solar domestic hot water (SDHW) control strategy employs on-off control of the collector fluid circulation pump, with a differential temperature sensing controller. When operated, the pump circulates the collector fluid at a relatively high constant flow rate approximately 50 l/hr-m^2 which results in a high value of the collector heat removal factor, F_R, and consequently, higher collector efficiency. There is, however, a thermal disadvantage associated with such high flow rates. With typically sized storage volumes (approximately 75 l/m^2), high-collector fluid flow rates cause the storage fluid to recirculate through the collector loop on the order of three to five tank turnovers per day. Both computer simulations and experiments [1, 2] have shown that a high degree of thermal stratification cannot be obtained with such recirculation rates.

Thermal stratification can be enhanced by reducing the collector fluid flow rate. Reducing the flow rate has two opposing effects. Lower flow rates result in lower values of F_R which reduce collector efficiency; but lower flow rates also result in less recirculation and a higher degree of stratification. This increased stratification results in lower collector inlet temperatures and thus increased collector efficiency. The increase in collector efficiency due to lower inlet temperatures often outweighs the decrease in efficiency due to the reduction in F_R, as first suggested by Tabor [3]. van Koppen [4] supports the existence of a reduced flow optimum using a simple two-node tank model, harmonically varying radiation and several simplifying assumptions. Veltkamp [5] uses a more detailed system model and presents results based on Dutch reference year weather data. Rademaker [6] suggests that the optimum occurs when only a slight amount of recirculation is allowed but that very near optimum performance is obtained when the collector flow rate is reduced just enough to avoid recirculation. Wang et al. [7] show

analytically and experimentally that the performance of a pumped SDHW system with no recirculation is comparable to that of a thermosyphon system. Both Rademaker's and Wang's conclusions are based on SDHW performance over short periods of time. Additional studies that investigate the performance tradeoffs between collector flow rate and tank stratification are reported by Mertol et al. [8], Robertson and Patera [9], Gordon and Zarmi [10], Collares-Pereira et al. [11], and Jesch and Braun [12].

This study supports the conclusions reached by others regarding the advantage of reduced collector flow rates using detailed TRNSYS [13, 14] simulations of SDHW systems under realistic operating conditions in several different climates of the United States. The sensitivity of the optimum fixed collector fluid flow rate to location, time of year, collector area and quality, preheat storage tank volume and energy losses, occurrence of mixing in the preheat storage tank, controller temperature deadbands, auxiliary set temperature, total daily load and load distribution are investigated. In addition to on/off operation with a fixed collector flow rate, the performance of constant storage volume systems using variable collector flow rates to achieve a fixed collector outlet temperature or fixed collector temperature rise, and variable flow rates based on the utilizable radiation are also examined.

2 System and Model Description

The two-tank SDHW system considered in this study is shown schematically in Fig. 1. The basic system specifications are as listed in Table 1 unless otherwise indicated. The auxiliary tanks contain two 4500 watt heating elements to boost the temperature of the solar preheated water if necessary. A tempering valve limits the temperature of the delivered water to the set temperature by mixing with mains water as needed. The mains temperature varies on a monthly basis from 8.2°C in January to 26.1°C in September with a value of 10.4°C in March. The storage tank environment temperature is a constant 21°C.
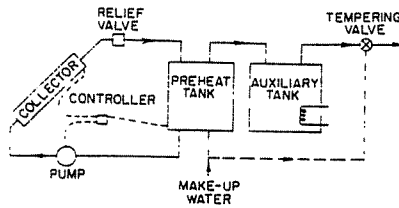
Fig. 1 Constant preheat storage volume system schematic

The collector performance is modeled with the Hottel-Whillier [15] equation:

$$Q_u = A_C[F_R(\tau\alpha)G_T - F_R U_L(T_i - T_a)]^+ \qquad (1)$$

where

Q_u = rate of useful energy gain
A_c = collector area
$F_R(\tau\alpha)$ = intercept of the collector efficiency versus $(T_i - T_a)/G_T$ curve (corrected for non-normal solar incidence)
G_T = solar radiation per unit area incident on collector plane
$F_R U_L$ = negative of the slope of the collector efficiency versus $(T_i - T_a)/G_T$ curve
T_i = collector inlet temperature
T_a = ambient temperature

The values of collector performance parameters $F_R U_L$ and $F_R(\tau\alpha)$ are affected by collector flow rate through the dependence of F_R on flow rate for unit area. Assuming the collector efficiency factor, F', and the collector loss coefficient, U_L, are independent of flow rate, $F_R U_L$ and $F_R(\tau\alpha)$ can be modified for any flow rate using an analytical correction ratio, r, derived in reference [16].

$$r = \cfrac{\dfrac{\dot{m}_C C_p}{A_C F' U_L}[1 - e^{-A_C F' U_L / \dot{m}_C C_p}]}{\left[\dfrac{\dot{m}_C C_p}{A_C F' U_L}[1 - e^{-A_C F' U_L / \dot{m}_C C_p}]\right]_{test}} \qquad (2)$$

where

$\dot{m}_C$ = collector fluid flow rate
C_p = collector fluid specific heat
F' = collector efficiency factor
U_L = collector loss coefficient

$F'U_L$ in both the numerator and denominator of equation (2) may be evaluated at the test flow rate using:

$$F'U_L = \frac{\dot{m}_C C_p}{A_C} ln\left[1 - \frac{A_C F_R U_L}{\dot{m}_C C_p}\right] \qquad (3)$$

At conventional flow rates (50 l/hr-m²), the flow through the absorber plate tubes is generally laminar, but the temperature profile may not be fully developed. Heat transfer relations for the developing region [17] give the heat transfer coefficient as a function of flow rate. For the base case collector considered in this study, the heat transfer coefficient at slow flow rates (approximately 10 l/hr-m²) was on the order of 30 percent less than for conventional collector flow rates. However, the magnitude of the fluid heat transfer coefficient, relative to the other factors such as bond conductance, etc., is such that F' is reduced by only 1 percent at slow collector flow rates.

Axial conduction in the absorber plate and variations in collector loss coefficient, due to axial temperature gradients were neglected in the collector model. The effect of these assumptions at reduced flow rates has been examined by Phillips [18]. Although these factors can have a significant effect on collector performance, they can be minimized with proper collector design.

Table 1 System parameters

| Description	Value
Base case collector:	
A_C	4.2 m²
$F_R(\tau\alpha)_{n\ test}$	0.805
$F_R U_{L\ test}$	4.73 W/m²°C
$\dot{m}_{C\ test}$	72 l/hr-m²
Incidence angle modifier	0.0989
Preheat tank:	
V_{PT}	303
U_{PT}	1.081 W/m²°C
Auxiliary tank:	
V_{AT}	151
U_{AT}	1.047 W/m²°C
T_{SET}	60°C
Load:	
volume, distributed over Rand Profile	300 l/day
Higher-quality collector:	
(corrected to $\dot{m}_C = 72$ l/hr-m²)	
$F_R(\tau\alpha)_n$	0.754
$F_R u_L$	3.62 W/m²°C
Lower-quality collector:	
(corrected to $\dot{m}_C = 72$ l/hr-m²)	
$F_R U_L$	8.57 W/m²°C
$F_R(\tau\alpha)_n$	0.697
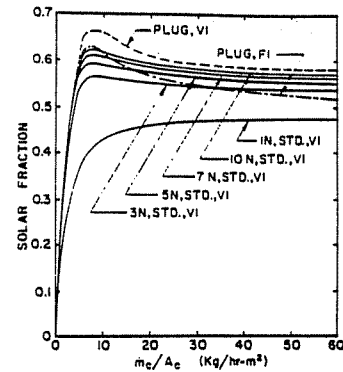
Fig. 2 Plug-flow versus multinode storage tank model comparison

For constant collector flow rate operation, an on-off differential controller is used to actuate the circulator pump when a temperature difference of 8.9°C exists between the collector outlet temperature and the temperature at the bottom of the storage tank. A temperature difference of less than 1.7°C causes circulation to cease.

When variable collector flow rate operation is used to obtain a specified collector outlet temperature or specified temperature rise across the collector, a new collector flow rate must be calculated each simulation time step. This flow rate is determined by first expressing the rate of useful energy collection as:

$$Q_u = \dot{m}_C C_p(T_o - T_i) \qquad (4)$$

where

T_o = collector outlet temperature

and then combining equations (1) and (2) and equating with equation (4)

$$\dot{m}_C = \frac{-F'U_L A_C}{C_p ln\left[1 - \dfrac{T_o - T_i}{(F_R(\tau\alpha)G_T/F_R U_L) - (T_i - T_a)}\right]} \qquad (5)$$

If, while in the fixed collector outlet temperature mode, the fluid in the bottom of the preheat storage tank reaches the specified collector outlet temperature, the pump turns off.

Varying the collector flow rate in proportion to the utilizable radiation (i.e, radiation above the critical level) requires advance information to avoid recirculation. A daily proportionality constant, C_1, was determined with a separate simulation in advance, such that the total daily collector flow would equal a specified amount, C_2.

$$C_2 = \frac{C_1}{\int_{\text{day}} (G_T - G_{T,c})^+ \, dt} \tag{6}$$

where

C_1 = total desired daily flow
C_2 = daily proportionally constant
$G_{T,c}$ = critical radiation level

The critical radiation level may be defined as the minimum amount of incident radiation for collector energy gains to overcome losses. Setting the useful energy gain to zero in equation (1) enables the critical radiation level to be expressed as:

$$G_{T,c} = \frac{F_R U_L (T_i - T_a)}{F_R (\tau\alpha)} \tag{7}$$

Multiplying the daily constant, C_2, by the actual instantaneous difference between the radiation incident on the collector and the critical threshold level yields the instantaneous collector flow rate, which when integrated over the day, very nearly gives the desired total daily flow, C_1.

The multinode storage tank model in Version 11 (and earlier versions) of TRNSYS [13] simulates tank thermal stratification by dividing the tank into a number of equally sized sections, or nodes. Veltkamp [5] has shown that to accurately model the performance of a stratified storage tank at low flow rates, as many as 60 nodes may be required. His conclusion is supported by simulation results in Fig. 2. These results are for Madison in May, but are typical of results obtained for other months and locations. The solid lines indicate the performance calculated for 1, 3, 5, 7, and 10 nodes. Progressively smaller increases in solar fraction are obtained as the number of nodes is increased. However, as the number of nodes increases, smaller simulation time steps are required, so simulations of SDHW performance with many nodes for extended periods are expensive.

Rather than using the existing TRNSYS tank model, the performance of the preheat tank was modeled using plug-flow tank model [14]. This model uses a number of variable size segments of fluid to model stratification. When collector flow occurs a uniform temperature segment of fluid (whose size depends on collector flow rate and simulation time step) is inserted into the tank profile at the appropriate location, thus shifting the position of all existing segments below the inlet. If a load flow occurs, the profile is again shifted by inserting a segment of fluid at the mains temperature and equal in size to the load flow during the time step. The segments and/or fraction of segments whose position falls outside the bounds of the tank are returned to the collector and/or load. The return temperatures are calculated based on a volume-weighted average. Storage energy losses/gains are then calculated individually for each segment. Each segment is assumed to be at a uniform temperature and interaction between segments due to conduction or convective mixing is not considered. Morrison and Braun [19] show that the effect of conduction in a vertical water storage tank is small. The effect of convective mixing is addressed in the following section. The advantage of the plug-flow model is that it does not need to solve systems of simultaneous differential equations as does the multinode model, and it is therefore much less costly to use.

The plug-flow model has two modes of operation. In mode 1, the tank has fixed inlet (*FI*) positions and any temperature inversions are eliminated by mixing with appropriate adjacent nodes. In mode 2, the tank has variable inlet (*VI*) positions and new segments are inserted at levels nearest to their own temperature which eliminates temperature inversions. If the inlet temperatures are within $0.5\,°C$ of an existing segment,
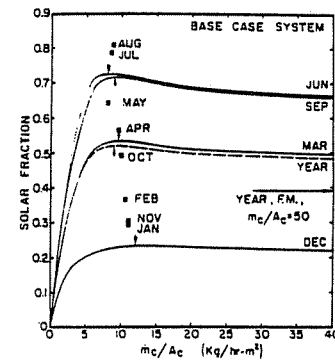

Fig. 3 Solar fraction versus collector flow rate per unit area for the base system in Madison
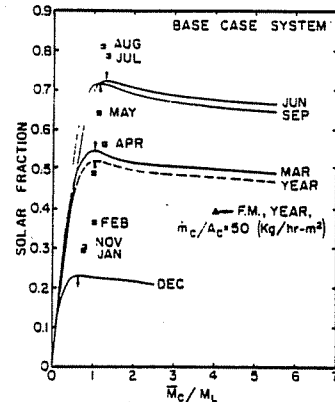

Fig. 4 Solar fraction versus the ratio of the monthly average daily total collector flow to daily local load flow for the base case system in Madison

the collector or load flow will combine with that segment, instead of creating a new one. The dotted lines in Fig. 2 show the results obtained for the base case system during a Madison May month for both modes of operation.

The variable inlet mode provides an upper limit on system performance because it allows the maximum possible thermal stratification. The results for a fully mixed preheat tank (1 node) provide the lower limit on performance. The fully mixed model will more accurately reflect actual performance when convective mixing is significant, as expected at high collector flow rates. As flow rate is decreased, convective mixing is reduced and actual performance should tend toward the predictions of the plug-flow model at a rate dependent on the tank design. An experimental study on this subject is underway at the National Bureau of Standards [20]. The results presented in this study were mainly generated using the variable inlet (mode 2) plug-flow model.

3 Results

Effect of Collector Flow Rate. Figure 3 shows the annual performance for the base case system in Madison, Wisc., using typical meteorological year (TMY) weather data [21]. Solar fraction is plotted versus collector fluid flow rate per unit collector area. The solar fraction is defined as the ratio of energy delivered by the solar system to the energy required to meet the load, including auxiliary tank energy losses. The yearly thermal optimum of 53.4 percent occurs at a collector fluid flow rate of 9 l/hr-m², which is about 20 percent of the conventional 50 l/hr-m². The stratified storage at this reduced flow rate results in an annual solar fraction which is 14.7 percentage points greater than that which would be achieved with a fully mixed preheat tank operating at conventional collector flow rates. All performance comparisons in this study are absolute improvements given in percentage points. Time of year has some effect on optimum flow rate. As day
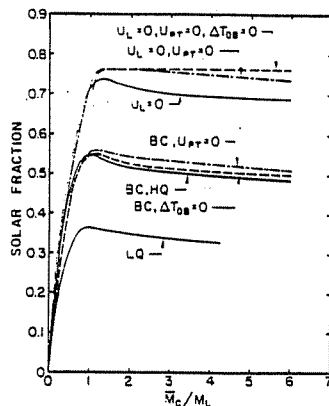
Fig. 5 Effect of collector loss coefficient, preheat storage losses and controller deadbands on base case system performance (March in Madison)
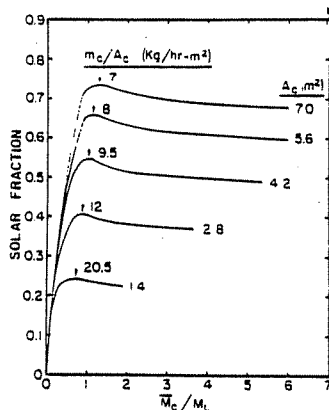

Fig. 6 Effect of collector area on base case system performance (March in Madison)

length, and thus pump operation time decrease, optimum flow rate increases. The monthly optimums are near the yearly optimum and the curves are fairly flat in the vicinity of the optimum. Thus, only a slight improvement could be realized by adjusting the flow rate on a monthly basis.

The same system was used to run annual simulations in both Seattle, Wash. and Albuquerque, N. Mex. In Seattle, the solar system provided approximately 43 percent of the annual load at an optimum collector flow rate of 9 l/hr-m^2, which is 11.5 percentage points above that provided by the system with a fully mixed storage tank operated at conventional flow rates. In Albuquerque, an annual solar fraction of 84 percent was obtained at a flow rate of 9 l/hr-m^2, which is 18.5 percentage points above fully mixed storage. An annual simulation was also run in Albuquerque using the same system but with one-half the collector area (2.1 m^2). This case resulted in an annual solar fraction of 52.5 percent at an optimum flow rate of 14 l/hr-m^2, which is a 12.6 percent improvement over the fully mixed system. Both the Seattle and Albuquerque results showed time of year dependence similar to that found in Madison.

Reduced Flow Rate. The results shown in Fig. 3 are replotted versus the ratio of monthly average daily total collector flow to daily total load flow ($\bar{M}_C/M_L$) and are shown in Fig. 4. The yearly optimum flow rate occurs very near to a $\bar{M}_C/M_L$ ratio of one. The optimum $\bar{M}_C/M_L$ ratios in the warmer months are slightly greater than one. This suggests that as radiation levels and ambient temperatures increase (and thus useful energy collection increases), system peformance can be improved slightly by allowing a small amount of recirculation.

The optimum $\bar{M}_C/M_L$ ratio for November, December, and

January falls below 1. A one-day analysis would indicate that the optimum ratio should never be below 1 (as shown by Rademaker [6]). However, on a monthly basis, the optimum ratio can fall below 1 due, in part, to day-to-day weather fluctuations. M_C is defined as the monthly "average" total daily collector flow; thus as the $\bar{M}_C/M_L$ ratio increases toward 1, too much recirculation may occur on the good days. The optimum $\bar{M}_C/M_L$ ratio is slightly affected by solar fraction, as shown in Fig. 4. System performance in March most nearly resembles the annual performance. The remainder of the results presented (unless otherwise indicated) will be for March in Madison, Wisc., but the same behavior exists when examined on an annual basis and in the other locations investigated.

Effect of Collector Quality, Tank Energy Losses, and Controller Settings. Figure 5 shows the effect of collector quality, preheat storage tank energy losses, and controller temperature deadbands on system performance. The base case collector, BC, is single-glazed with a selective surface absorber. The higher quality collector, HQ, is double-glazed with a selective surface absorber and the lower quality collector, LQ, has one cover with a flat black absorber plate. The performance characteristics are listed in Table 1. The base case collector and the higher quality collector yielded nearly identical performance and are represented as one curve in Fig. 5. The collector quality has very little effect on the optimum $\bar{M}_C/M_L$ ratio, but the optimum flow rate per unit area does increase slightly with increased collector quality because the collector operating time increases. Removing preheat storage tank losses from the base case system improves performance slightly and increases the optimum $\bar{M}_C/M_L$ ratio from 1 to 1.15. With a zero tank loss coefficient, the colder fluid at the bottom of the tank cannot receive any gains from the environment. Thus, the average bottom of the tank temperature during collector on time is lower and the collector operates longer, causing the $\bar{M}_C/M_L$ to increase slightly at low collector flow rates. Setting the differential controller temperature deadbands to zero has the effect of shifting the base case curve to slightly higher $\bar{M}_C/M_L$ ratios. The zero-degree deadbands cause the circulation pump to operate whenever the ambient temperature is greater than or equal to the temperature at the bottom of the preheat tank.

Figure 5 also shows the performance that could be obtained with systems having no collector or tank thermal losses. If a collector had a loss coefficient of zero, a reduced flow rate optimum should not exist because the collector performance would be independent of temperature. However, as indicated by Fig. 5 an optimum does exist for the particular system investigated at a reduced flow rate. This optimum occurs partly because the net preheat storage tank losses increase with flow rate, thus reducing the net energy delivered by the solar system at higher flow rates. When the preheat tank loss coefficient is set to zero, however, a reduced flow rate optimum still exists. The differential controller used in the base case simulation had a 8.9°C deadband upper limit and a 1.7°C deadband lower limit, which reduced the energy collection more at higher flow rates than at lower flow rates. As shown in Fig. 5, when the temperature deadband is set to zero with both a collector loss coefficient of zero and a tank loss coefficient of zero, the performance curve is flat and a reduced flow rate optimum does not exist.

Effect of Collector Area. Figure 6 shows the effects on performance of varying the collector area while the rest of the system remains unchanged. The optimum $\bar{M}_C/M_L$ ratio increases slightly with both A_C and solar fraction. The optimum total collector flow rate also increases with A_C, but the
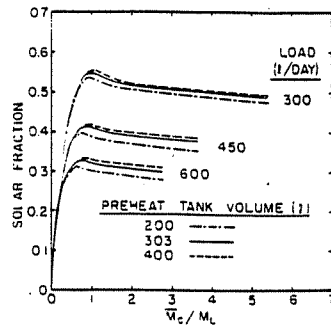
Fig. 7 Effect of total daily draw and preheat storage volume on base case system performance (March in Madison)
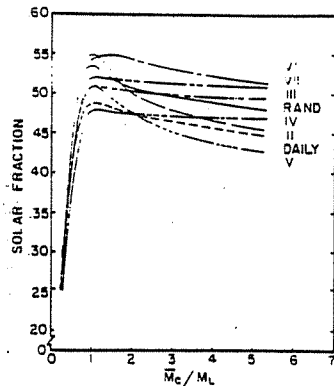

Fig. 8 Effect of load distribution on base case system performance (March in Madison)

optimum collector flow rate per unit area decreases with increasing collector area.

· An optimum collector flow rate exists at reduced flow rates primarily because the reduction in collector efficiency due to a reduction in F_R is more than compensated for by the increase in collector efficiency resulting from reduced collector fluid inlet temperatures. Collector fluid inlet temperature is a function of the total collector flow rate, while F_R is dependent on flow rate per unit area, as shown in reference [16]. This dependence of F_R on flow rate per unit area explains the location of the optimums in Fig. 6. At a collector area of 1.4 m^2, the optimum $\bar{M}_C/M_L$ is approximately 0.75 with a flow rate of 20.5 l/hr·m^2. Any increase in flow rate above this value will not produce an accompanying increase in F_R great enough to overcome the reduction in collector efficiency resulting from an increased collector inlet temperature. The optimum $\bar{M}_C/M_L$ ratio of the larger collector areas is slightly greater than one because they operate at lower flow rates per unit area. In this case, an increase in collector flow rate causes a large enough increase in F_R to outweigh its accompanying increase in collector inlet temperature.

Effect of Load Draw and Storage Volume. Figure 7 shows the effect of varying the total daily load on system performance for three different preheat storage tank volumes. The optimum $\bar{M}_C/M_L$ ratio for all tank sizes decreases slightly as the total daily draw increases.

The $\bar{M}_C/M_L$ ratio may not be the only important variable for storage tank sizes which are smaller than the average daily load. The optimum total daily collector flow is on the order of the load flow, unless the tank volume and load flow during collector on-time are not large enough to avoid recirculation. The optimum $\bar{M}_C/M_L$ ratios are less than 1 for the 450 and 600/day loads because of this recirculation limitation. For a fixed value of $\bar{M}_C/M_L$, the load flow during collector on time increases in proportion to the total daily load flow. However, with a fixed tank volume, the total collector flow can only increase by an amount equal to the increase in load flow

Table 2 Variation in daily load draw for day-to-day profile

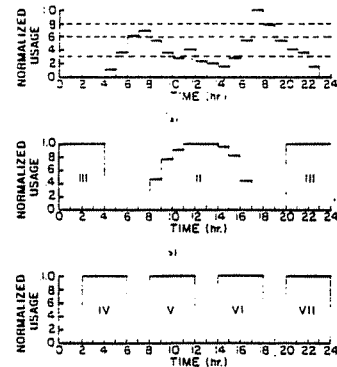|		Percentage of Weekly Total				
Sun.	Mon.	Tues.	Wed.	Thur.	Fri.	Sat.
5.7	42.9	2.8	2.8	14.4	2.8	28.6

Fig. 9 Load distributions: (a) RAND, (b) 8 PM–4 AM constant and proportional to monthly radiation distribution, and (c) 2–6 AM, 8–12 AM, 2–6 PM, and 8–12 PM constant

during collector on-time, while still avoiding recirculation. When the recirculation limitation is encountered, the optimum collector flow becomes independent of any load flow during collector off time. Thus, the optimum ratio of $\bar{M}_C/M_L$ decreases. A comparison of the 450 and 600 l/day curves for preheat tank volumes of 200, 300 and 400 liters shows that smaller tank volumes cause the recirculation limit to be encountered at lower $\bar{M}_C/M_L$ ratios.

Effect of Load Distribution. Figure 8 shows the effect of varying the load distribution. Seven hourly load profiles and one day-to-day profile were investigated. The base case distribution was the RAND [22] profile which is shown in Fig. 9(a). Curve II represents the performance of profile II shown in Fig. 9. The load is proportional to the monthly radiation distribution and occurs only during collector on-time. Curves III–VII represent constant load draws between the hours indicated in Figs. 9(b) and (c). The RAND profile and profiles II–VII are repeated each day. The day-to-day distribution represents a weekly cycle using the RAND profile each day with the total daily draw varying each day (as shown in Table 2), such that the load equals 2100 liters/week.

The variation in performance with load distribution is caused by better matching of some profiles to incident radiation and by the amount of nighttime preheat storage losses. Loads III, IV, and VII have much flatter curves than the other profiles because they occur during collector off-time and thus do not affect when recirculation occurs. The largest portion of the variation in performance between profiles is due to the existence of stratification. The effect of load distribution in fully mixed systems has been examined analytically by Buckles and Klein [23] and experimentally by Fischer and Fanney [24]. Their results showed variation in hourly load profile to have little effect on fully mixed system performance at high-collector flow rates. All of load profiles investigated in this study have optimum $\bar{M}_C/M_L$ ratios near 1 except profile VI which has a slightly higher optimum $\bar{M}_C/M_L$ ratio of approximately 1.4. This is due to the insertion of 300 liters of mains water into the bottom of the preheat storage tank in the afternoon, which allows the total daily collector flow to be greater, while still avoiding recirculation.

In all simulations, the RAND load profile was obtained by varying the load flow rate each hour and keeping that flow rate constant over the entire hour. It could also have been achieved by keeping the load flow rate constant at a specified value and varying the duration of time of each step in the
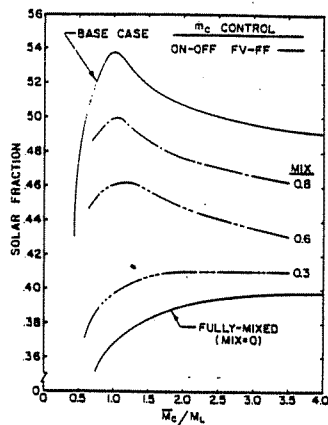
Fig. 10 Effect of convective mixing on base case system performance (March in Madison)
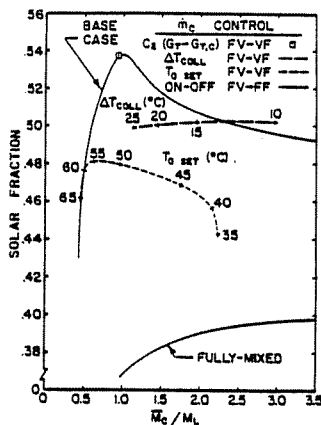

Fig. 11 Comparison of variable collector flow rate control alternatives for fixed volume (FV) systems with fixed (FF) or variable (VF) collector flow

profiles. Comparison of these two methods showed a very small difference in system performance (on the order of 0.1 percent). If the storage tank model accounted for the effects of internal mixing due to load flow, the differences between these two methods would show a greater effect on system performance.

Effect of Convective Mixing. System performance at reduced collector fluid flow rates highly depends on the degree of the thermal stratification in the preheat storage tank. Figure 10 shows the effect on system performance of various degrees of mixing in the preheat tank. All curves were generated using the variable inlet plug-flow tank model except the curve labeled "FULLY MIXED" which was obtained using the tank model with one node. The curve labeled "BASE CASE" represents the perfectly stratified preheat tank. The MIX equal 0.8 curve represents the performance of a system whose preheat tank was completely mixed each time the normalized load draw was greater than or equal to 0.8. This occurs once per day as shown in Fig. 9(a). Similarly the MIX equal 0.6 and 0.3 curves correspond to systems whose preheat tank was completely mixed each time the normalized load was greater than or equal to 0.6 and 0.3, respectively. Thus the 0.6 and 0.3 curves represent successively greater frequencies of complete mixing, which is also shown in Fig. 9.

As the frequency of complete mixing increases, system performance drops. The 0.8 and 0.6 curves still show a reduced collector flow rate optimum near $\bar{M}_C/M_L = 1$, but the low $\bar{M}_C/M_L$ optimum disappears for the MIX equal 0.3 curve. A plug-flow tank simulation was also run at MIX equal zero which completely mixes the preheat storage every time step. The results, as expected, fall directly on top of the fully

mixed results. These curves are not intended to represent what actually happens during load flow (i.e., complete mixing of preheat storage tank), but rather to give an approximation of system performance with less than perfect stratification. These results show the strong dependence of system performance on a high degree of thermal stratification. However, when a thermal optimum is present, it always occurs near $\bar{M}_c/M_c$ equal to 1.

Effect of Auxiliary Set Temperature. The effect of auxiliary set temperature on system performance was examined by performing additional simulations at set temperatures of 50°C and 40°C. The optimum $\bar{M}_C/M_L$ ratio increases slightly with solar fraction, and with decreasing set temperature. The optimum flow rate per unit area also eases slightly as the optimum $\bar{M}_C/M_L$ ratio increases. However, the effect of auxiliary set temperatures is small in the range examined.

Effect of Variable Collector Flow Rate. Figure 11 compares the performance of three different variable collector flow rate control strategies to the performance of a fixed collector flow rate system with on-off temperature differential control. The fixed collector outlet temperature mode has a maximum solar fraction of 48.1 percent at an optimum $\bar{M}_C/M_L$ of 0.62 which corresponds to a collector set temperature of 55°C. This is a 7.3 percent improvement over a fully mixed system operating at 50 l/hr-m², but it is still 5.7 percent lower than the optimum performance of the reduced fixed flow rate system. The fixed collector temperature rise mode of control has a maximum solar fraction of 50.3 percent which is still 3.5 percent lower than the reduced fixed flow rate system.

Collares-Pereira et al. [25] have also found that systems with variable flow rate control perform worse than constant flow rate systems when there is no recirculation. As they show, this result can be explained by considering the utilizable radiation for variable and constant flow rate control. To achieve a specified collector outlet temperature or collector temperature rise, a minimum amount of radiation is required. Taking the limit of equation (4) as useful energy gain tends toward zero causes the collector flow rate to go to zero because the collector inlet and outlet temperatures are fixed. Taking the limit as $\dot{m}_c$ goes to zero in equation (5) allows this minimum required radiation, $G_{T,\text{min}}$ to be determined as:

$$G_{T,\text{MIN}} = \frac{(T_o - T_a)F_R U_L}{F_R(\tau\alpha)} \qquad (8)$$

This minimum radiation level has the same form as the critical level in equation (7), except that T_o, the collector fluid outlet temperature, appears in place of T_i. The critical level for fixed outlet temperature or fixed temperature rise operation is thus higher than that for constant flow operation. As a result, collector on-time is shorter (thus reducing useful energy collection), and system performance is less than that which could be achieved with a reduced fixed flow rate system. As the specified collector outlet temperature or temperature rise set points are reduced (which lowers the $G_{T,\text{MIN}}$ levels), recirculation begins to inhibit system performance.

Variable flow rate control in proportion to the utilizable radiation results in a solar fraction of 53.7 percent. This is approximately equal to the optimum reduced fixed flow rate system performance. However, optimal control using this strategy requires advance knowledge of weather conditions which makes practical application difficult.

4 Discussion and Conclusions

When conventional SDHW systems are operated at reduced fixed collector fluid flow rates (on the order of 20 percent that

of conventional flow rates) a higher degree of thermal stratification can be achieved in the preheat storage tank. The resulting increase in collector efficiency due to reduced collector inlet temperatures often outweighs the reduction in collector efficiency due to the lower values of F_R. System performance is also enhanced slightly by the reduction in preheat storage tank losses resulting from reduced collector fluid flow rates. For the particular reduced constant flow rate systems investigated, the annual performance with stratified storage at reduced flow rates showed an absolute improvement from 11.5 to 14.7 percentage points greater than that which would be achieved with fully mixed storage tanks operating at conventional collector flow rates.

The fixed collector outlet temperatures and fixed collector temperature rise variable flow rate strategies showed absolute improvements of percentage points 7.3 and 9.5 percent, respectively, when compared to fully mixed systems operating at conventional constant flow rates. Both strategies however performed worse than the simpler reduced constant flow rate, on-off differential temperature control. Proportional control based on the utilizable radiation (ie., level of incident radiation above the critical level) performed very nearly as well as the optimum reduced constant flow rate strategy. This method requires knowledge of future weather conditions which makes practical application difficult.

Parasitic power requirements were neglected in this investigation. However, if they were included, the reduced collector flow rate system would show an even greater relative improvement over conventional high flow rate systems.

The optimum system performance occurs very near to a monthly average daily total collector flow to daily total load flow ($\dot{M}_C/M_L$) ratio of one. The optimum $\dot{M}_C/M_L$ ratio shows some time of year dependence but this is due mainly to day length variations. The optimum collector flow rate per unit area is less dependent on time of year and thus only a slight improvement in performance could be realized by adjusting the collector flow on a monthly basis.

Fixed controller temperature deadbands were found to reduce system performance slightly at higher flow rates, thus increasing the relative difference in performance between low and high flow rate systems.

Collector area and quality, preheat storage energy losses, and auxiliary set temperature all had some effect on solar fraction but showed very little effect on the optimum $\dot{M}_C/M_L$ ratio.

The storage tank volume, daily load, and load distribution have a direct effect on the optimum fixed flow rate, because of their impact on the occurrence and amount of recirculation. The optimum $\dot{M}_C/M_L$ ratio ranged from 0.6 to 1.4 for the range of parameters examined.

6 References

1 Cole, R. L., and Bellinger, J. O., "Natural Thermal Stratification Tanks," Argonne National Lab, 82-5, Feb. 1982.

2 Fanney, A. H., and Klein, S. A., "Performance of Solar Domestic Hot Water Systems at the National Bureau of Standards—Measurements and Predictions," ASME JOURNAL OF SOLAR ENERGY ENGINEERING, Vol. 105, 1983.

3 Tabor, H., "A Note on the Thermosyphon Solar Hot Water Heater," COMPLES, Vol. 33, No. 17, 1969.

4 van Koppen, C. W. F., et al., "The Actual Benefits of Thermally Stratified Storage in a Small and a Medium Size Solar System," Proc. ISES, Atlanta, May, 1979.

5 Veltkamp, W. B., "Thermal Stratification in Heat Storage," in: C. den Ouden, Thermal Storage of Solar Energy, Martinus Nijhoff, The Hague, Vol. 2, No. 6, 1980.

6 Rademaker, O., "On the Dynamics of (Thermal Solar) Systems Using Stratified Storage," in C. den Ouden, Thermal Storage of Solar Energy, Martinus Nijhoff, The Hague, Vol. 2, No. 6, 1980.

7 Wang, Y. F., Li, Z. L., and Sun, X. L., "A 'Once Through' Solar Water Heating System," Solar Energy, Vol. 29, 1982, pp. 541-547.

8 Mertol, A., Place, W., Webster, T., and Greif, F., "Detailed Loop Model Analysis of Liquid Solar Thermosyphons With Heat Exchangers," Solar Energy, Vol. 27, 1981, pp. 367-386.

9 Robertson, H. S., and Patera, R. P., "Collection of Solar Energy at Specified Output Temperature," Solar Energy, Vol. 29, No. 4, 1982, p. 331.

10 Gordon, J. M., and Zarmi, Y., "Thermosyphon Systems: Single vs Multi-Pass," Solar Energy, Vol. 27, No. 5, 1981, p. 441.

11 Collares-Pereira, M., Gordon, J. M., Rabl, A., and Zarmi, Y., "Design and Optimization of Solar Industrial Hot Water Systems With Storage," Solar Energy, Vol. 32, 1984, pp. 121-133.

12 Jesch, L. F., and Braun, J. E., "Variable Volume Storage and Stratified Storage for Improved Water Heater Performance," submitted to Solar Energy 1982.

13 University of Wisconsin-Madison Solar Energy Laboratory, TRNSYS 11.1, EES Report 38-11, 1981.

14 University of Wisconsin-Madison Solar Energy Laboratory, TRNSYS 12.1, EES Report 38-11, 1983.

15 Hottel, H. C., and Whillier, A., "Evaluation of Flat-Plate Collector Performance," Trans. of Conf. on Use of Solar Energy, Part 1, Vol. 74, University of Arizona Press, 1958.

16 Duffie, J. A., and Beckman, W. A., Solar Engineering of Thermal Processes, Wiley Interscience, New York, 1980.

17 Kays, W. M., and Crawford, M. E., Convective Heat and Mass Transfer, 2nd edition, McGraw-Hill, New York, 1980.

18 Phillips, W. F., "The Effects of Axial Conduction on Collector Heat Removal Factor," Solar Energy, Vol. 23, 1979, p. 187.

19 Morrison, G. L., and Braun, J. E., "System Modelling and Operation Characteristics of Thermosyphon Solar Water Heaters," submitted to Solar Energy, 1984.

20 Fanney, A. H., National Bureau of Standards, Gaithersburg, Maryland.

21 Hall, I. J., et al., "Generation of a Typical Meteorological Year," Sandia National Laboratory, Report SAND78-1601, 1978.

22 Mutch, J. J., "Residential Water Heating, Fuel Consumption Economics and Public Policy, RAND, Dept. R1498, NSF, 1974.

23 Buckles, W. E., and Klein, S. A., "Analysis of Solar Domestic Hot Water Heaters," Solar Energy, Vol. 27, May, 1980, p. 417.

24 Fisher, R. A., and Fanney, A. H., "Thermal Performance Comparisons for a Solar Hot Water System Subjected to Various Hot Water Load Profiles," in review, ASME.

25 Collares-Pereira, M., Gordon, J. M., and Zarmi, Y., "Constant Sensible Heat Load Applications Variable vs Constant Flow Solar Systems," Solar Energy, Vol. 32, 1984, pp. 135-137.